

ARTICLE



ACUTE MYELOID LEUKEMIA

The epigenetic state of the cell of origin defines mechanisms of leukemogenesis

Zhiheng Li^{1,2,3}, Sara Fierstein ^{1,2}, Mayuri Tanaka-Yano ^{1,2}, Katie Frenis ^{1,2}, Chun-Chin Chen^{1,2}, Dahai Wang^{1,2}, Marcelo Falchetti ⁴, Parker Côte⁵, Christina Curran^{1,2}, Kate Lu⁵, Tianxin Liu², Stuart Orkin^{2,6,7}, Hojun Li^{5,8}, Edroaldo Lummertz da Rocha ⁴, Shaoyan Hu ³✉, Qian Zhu ^{9,10}✉ and R. Grant Rowe ^{1,2,7,10}✉

© The Author(s), under exclusive licence to Springer Nature Limited 2024

Acute myeloid leukemia (AML) shows variable clinical outcome. The normal hematopoietic cell of origin impacts the clinical behavior of AML, with AML from hematopoietic stem cells (HSCs) prone to chemotherapy resistance in model systems. However, the mechanisms by which HSC programs are transmitted to AML are not known. Here, we introduce the leukemogenic *MLL-AF9* translocation into defined human hematopoietic populations, finding that AML from HSCs is enriched for leukemic stem cells (LSCs) compared to AML from progenitors. By epigenetic profiling, we identify a putative inherited program from the normal HSC that collaborates with oncogene-driven programs to confer aggressive behavior in HSC-AML. We find that components of this program are required for HSC-AML growth and survival and identify RNA polymerase (RNAP) II-mediated transcription as a therapeutic vulnerability. Overall, we propose a mechanism as to how epigenetic programs from the leukemic cell of origin are inherited through transformation to impart the clinical heterogeneity of AML.

Leukemia; <https://doi.org/10.1038/s41375-024-02428-y>

INTRODUCTION

Acute leukemias show variation in their differentiation lineages, states of maturation, and oncogenic driver mutations. This biologic heterogeneity translates into variable susceptibility to chemotherapy and risk of relapse that together contribute to persistent disparities in outcome. In AML, differences in outcome tracking with underlying biology persist despite the development of increasingly effective risk-stratified chemotherapy regimens, indicating that the factors affecting prognosis are not fully understood. Principles of tissue stem cell biology have been previously applied to the study of AML LSCs – the rare leukemic cells that fuel AML growth and relapse – but the inherent stochasticity of leukemic cellular ontogenies and plasticity of the LSC state have hindered the development of therapeutic strategies targeting LSCs, challenging efforts to translate such therapies to the clinic [1–3]. However, retention or activation of stem cell programs is a significant and reproducible adverse factor affecting outcomes in leukemia [4–6].

Normal HSCs reside at the apex of the hematopoietic hierarchy, uniquely maintaining the ability to self-renew to fully reconstitute the entire hematopoietic system – properties that are lost during progression through hematopoietic differentiation [7]. In normal

hematopoiesis, self-renewal is encoded within the HSC epigenome; therefore, it is reasonable to hypothesize that such an epigenetic program is maintained through the process of leukemogenesis to define LSCs and impact AML behavior [8]. Indeed, it has been previously demonstrated that the normal hematopoietic cell of origin impacts the biology of experimentally derived AML, with AML derived from HSCs and multipotent progenitors (MPPs) behaving more aggressively compared to that derived from downstream, lineage-restricted progenitors, consistent with relative enrichment of LSC programs [5, 9, 10].

Experimentally, LSCs are detected by their ability to engraft immunodeficient mice and initiate transplantable lethal leukemia [11–14]. LSCs within any individual leukemia can be heterogeneous – they can vary in their differentiation state, transcriptomes, and patterns of surface marker expression [2, 3, 6, 15]. Moreover, the LSC state can be plastic, likely contributing to the lack of success of LSC-targeted therapies [3, 15, 16]. Leukemic cellular ontogeny therefore departs drastically from that of normal hematopoiesis – in leukemia, the LSC state exists at multiple hierarchical levels, with stem cell epigenetic and transcriptional programs the only common factor between phenotypically heterogeneous LSCs. At the clinical level, the fundamental HSC

¹Stem Cell Program and Stem Cell Transplantation Programs, Boston Children's Hospital, Boston, MA, USA. ²Department of Hematology/Oncology, Boston Children's Hospital, Boston, MA, USA. ³Department of Hematology/Oncology, Children's Hospital of Soochow University, Suzhou, Jiangsu, China. ⁴Federal University of Santa Catarina, Florianopolis, Brazil. ⁵Massachusetts Institute of Technology, Cambridge, MA, USA. ⁶Howard Hughes Medical Institute, Boston, MA, USA. ⁷Harvard Medical School, Boston, MA, USA.

⁸Department of Pediatrics, University of California, San Diego, CA, USA. ⁹Baylor College of Medicine, Department of Molecular and Human Genetics, Houston, TX, USA. ¹⁰These authors contributed equally: Qian Zhu, R. Grant Rowe. ✉email: hushaoyan@suda.edu.cn; qian.zhu@bcm.edu; Grant_rowe@dfci.harvard.edu

Received: 23 April 2024 Revised: 18 September 2024 Accepted: 24 September 2024

Published online: 01 October 2024

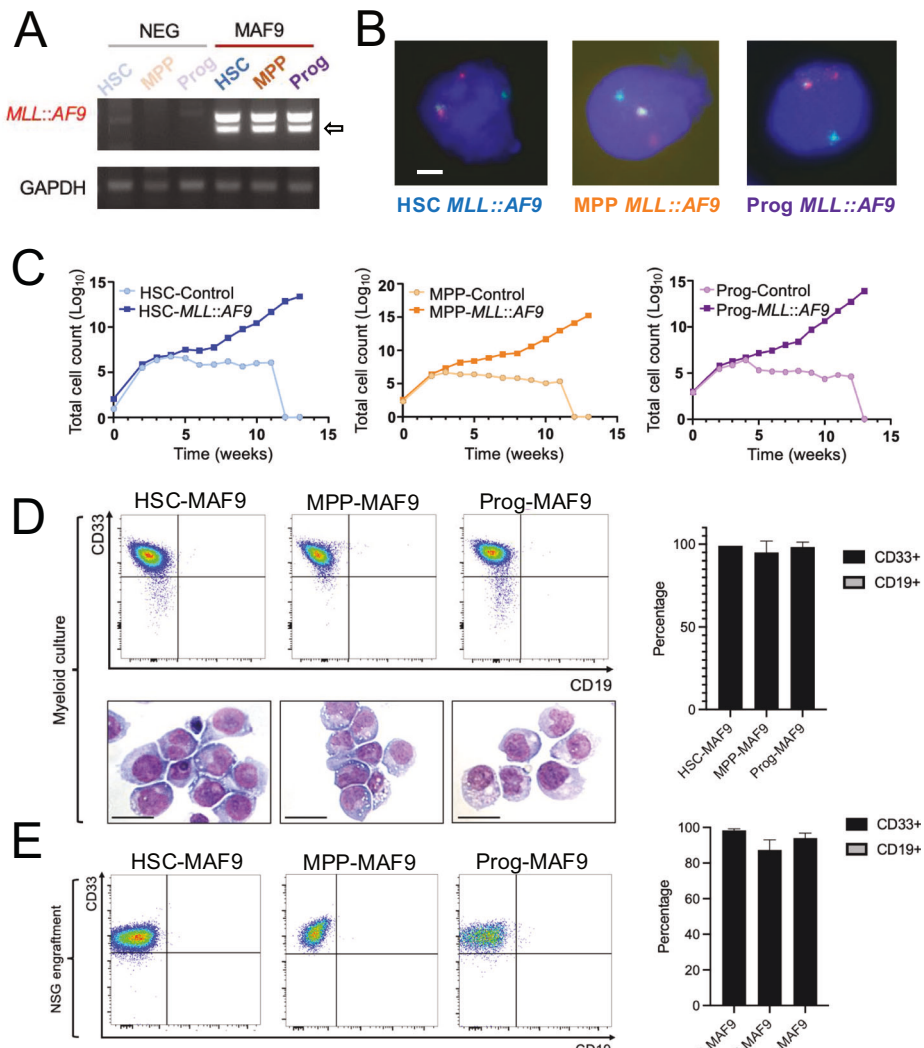


Fig. 1 Generating AML of defined cellular origin by engineering the *MLL-AF9* translocation in human HSCs. A RT-PCR results showing specificity of the *MLL-AF9* fusion gene to the conditions that had undergone editing. Arrow indicates skipping of exon 11 of *MLL-AF9*. **B** FISH for an *KMT2A*/11q23 breakapart probe demonstrating breakage of the *KMT2A/MLL1* locus in edited AML cells (scale = 10 μ m). **C** Two days following editing of the *MLL1* and *AF9* loci or control editing, HSCPs were sorted into the indicated fractions and growth monitored over time (representative results from one donor shown, see also Fig. S1F). **D** Representative immunophenotyping and morphology of leukemias of the indicated origins under myeloid growth conditions (results presented at mean \pm SEM, comparisons all non-significant by one-way ANOVA, $n = 3$ independent experiments; scale = 30 μ m). **E** Immunophenotyping of AMLs of defined cellular origins developed upon transplantation into NSG mice (results presented at mean \pm SEM, comparisons all non-significant by one-way ANOVA, $n = 4\text{--}5$ mice per condition).

property of self-renewal must be maintained in LSCs to support leukemia growth and to trigger relapse [16]. It would therefore follow that these properties must be epigenetically retained (in leukemia derived from HSCs) or ectopically gained by the activity of oncogenes (in leukemia derived from non-self-renewing progenitors). The mechanisms by which this occurs are not well understood.

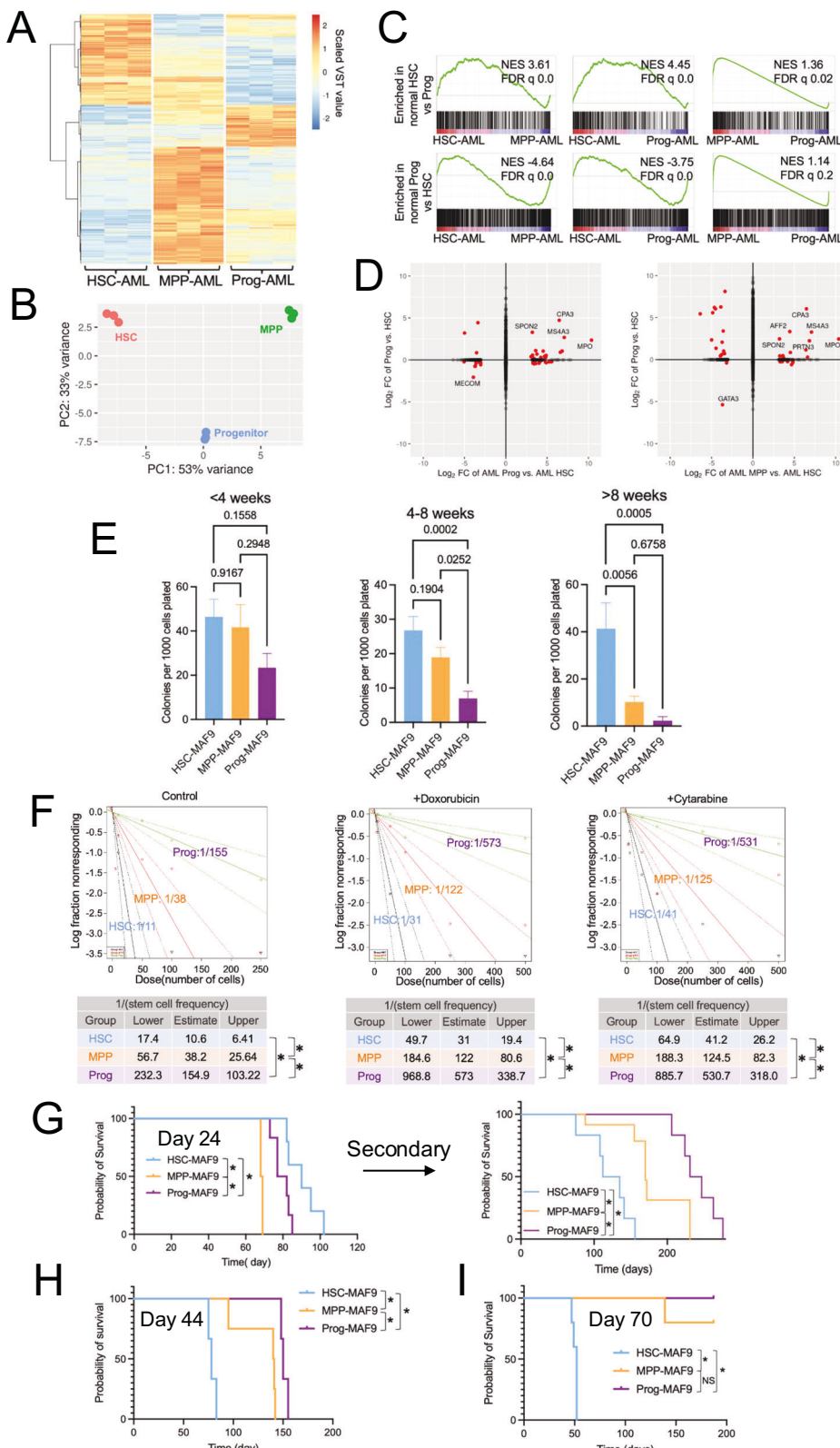
In this study, we adapted and optimized a model of gene editing using CRISPR/Cas9 to engineer the *MLL-AF9* chromosomal translocation that drives leukemogenesis into primary human neonatal HSCs and progenitors (HSPCs) [17]. We then sort various defined HSPC populations and place them in conditions that favor transformation to AML, thus deriving human AMLs with defined cells of origin [18]. Using epigenetic profiling, we defined a putative core *MLL-AF9*-driven program common to all cells of origin, as well as oncogene-driven programs dependent on the epigenetic state specific to each cell of origin. We also uncover oncogene-independent, putatively inherited epigenetic programs

from each cell of origin. Within the HSC-specific epigenetic program, we find that HSC-AML depends on RNAP II-mediated transcription and splicing relative to AML from progenitors. While HSC-AML is relatively resistant to conventional chemotherapy, this program confers sensitivity to inhibition of RNAP II-mediated transcription and splicing inhibition. Overall, by tracing inheritance of epigenetic programs through transformation we define therapeutic vulnerabilities in LSCs of HSC origin.

RESULTS

Cell of origin impacts AML LSC state

To understand mechanisms of implementation of the LSC state in acute leukemia, we adapted a CRISPR/Cas9-based editing approach to engineer the *MLL-AF9* oncogene in human umbilical cord blood HSPCs (Fig. S1A–C) [17]. Following editing of bulk CD34 $^{+}$ HSPCs, we used fluorescence activated cell sorting to derive leukemias of defined origin (HSC (Lineage $^{-}$ CD34 $^{+}$ CD38 $^{-}$



CD45RA⁻ CD90⁺), MPP (Lineage⁻ CD34⁺ CD38⁻ CD45RA⁻ CD90⁻), and progenitor (Prog; Lineage⁻ CD34⁺ CD38⁺) and confirmed the presence of the *MLL-AF9* fusion oncogene in the resulting AMLs derived under pro-myeloid culture conditions (stem cell factor (SCF), FLT3 ligand (FLT3L), thrombopoietin (TPO),

interleukin-3 (IL-3), and interleukin-6 (IL-6); Fig. 1A, B, S1D–E). Compared to HSPCs that underwent sham editing, HSPCs expressing *MLL-AF9* showed sustained proliferation in culture, consistent with a transformed phenotype (Fig. 1C, S1F). AMLs uniformly showed an immature myelomonocytic phenotype and

Fig. 2 Retention of stemness programs in HSC leukemia. Gene expression profiling of derived HSC-AML, MPP-AML, and Prog-AML with heatmap (**A**) scaled variance stabilizing transformation (VST) value) and principal component analysis (**B**). **C** Gene set enrichment analysis (GSEA) for the indicated human signatures (Table S2) [19] with normalized enrichment score (NES) and false discovery rate q (FDR q) value shown. **D** Correlation of transcripts between normal HSCs and progenitors [21] and the indicated AML comparisons. **E** CFU assays at the indicated time windows post *MLL-AF9* editing. Results comparing individual experiments by one-way ANOVA with *p*-values shown for the indicated comparisons ($n=7\text{--}15$ biologic replicates for each condition from cultures from at least three individual donors). **F** LT-IC assays were performed with AML cultures of defined origins under control conditions or with the indicated drug exposures (10 nM doxorubicin or 100 nM cytarabine) and results compared by limiting dilution analysis with significant differences (* $p < 0.0001$) by χ^2 testing indicated ($n=4$ independent experiments/initial cultures from at least two independent HSPC donors pooled in each analysis). **G-I** Myeloid leukemia cultures of defined cellular origins were xenotransplanted into NSG mice at the indicated time points following transformation, and survival of each cohort monitored. In panel **G**, cells from terminal AMLs isolated from the day 24 xenotransplant were secondarily transplanted and survival monitored in recipients (results compared by log-rank test with * indicating $p < 0.05$). Each transplant was from an independent culture, and results include two independent HSPC donors.

aberrant surface marker profile with co-expression of CD117 with CD14 and CD11b that was maintained upon xenotransplantation (Fig. 1D-E, S2A). Compared to sham-edited cells, AMLs activated expression of canonical *MLL-AF9* target genes (Fig. S2B).

Using RNA sequencing, we found that AMLs of defined origins maintained distinct transcriptional profiles, and that HSC-AML maintained a human HSC signature relative to MPP- and Prog-AML, while MPP- and Prog-AML maintained a progenitor signature relative to HSC-AML (Fig. 2A-C, Table S1-2) [19]. MPP-AML maintained an HSC signature relative to Prog-AML, although this was to a weaker degree compared to HSC-AML, and there was no significant enrichment in the progenitor signature between MPP-AML and Prog-AML (Fig. 2C). By comparing to normal benchmark HSPC transcriptomes, we found that both MPP-AML and Prog-AML maintain signatures of myeloid differentiation relative to HSC-AML, including expression of *MPO*, *MS4A3*, and *CPA3* (Fig. 2D) [20, 21]. Within the first 28 days following editing and early in transformation, as a marker of LSC content, AMLs of each cell of origin showed similar clonogenesis in methylcellulose culture; however, continued culture under myeloid conditions resulted in relative loss of clonogenic potential in AMLs derived from MPPs and progenitors relative to AML from HSCs, consistent with persistence of self-renewal of LSCs in HSC-AML (Fig. 2E). Accordingly, long-term initiating cell (LT-IC) assays demonstrated higher culture initiating cell content in HSC- and MPP-AML compared to progenitor-AML, and HSC-AML initiating cells persisted in the presence of cytarabine and doxorubicin – the drugs used in upfront therapy for AML – compared to AMLs of MPP and progenitor origin (Fig. 2F).

As the gold-standard assay for LSC function, we performed xenotransplantation in immunodeficient NSG mice. Early following transformation (day 24), we observed similar capacity to generate terminal leukemia from each origin (Fig. 2G). However, secondary xenotransplantation showed that HSC-AML most robustly maintained self-renewing LSC content, followed by MPP-AML (Fig. 2G). In accordance with findings in clonogenesis assays, HSC-AML from later periods in culture following editing (days 44 and 70) were consistently most efficient in engrafting and generating terminal AML (Fig. 2H, I). AMLs from early time points following transformation were generally polyclonal, while engraftment from later time points was monoclonal, consistent with selection for self-renewing LSC clones (Fig. S2C). Together, these findings indicate that LSC properties are most robustly maintained in AML of HSC origin.

MLL-AF9 genomic localization based on the cell of origin

There are two mechanistic possibilities to explain the differential behavior of AMLs of each origin despite equivalent expression of the driver oncogene – cell of origin-specific effects of *MLL-AF9* in implementing leukemic programs, or epigenetic inheritance of stem cell programs from the cell of origin independently of *MLL-AF9*. To test this idea, we performed epigenetic profiling using Cleavage Under Targets and Release Using Nuclease (CUT&RUN) in

AMLs of defined origin [22]. Our strategy was to distinguish loci bound by the *MLL-AF9* fusion and/or wild-type *MLL1/KMT2A* in the background of markers of chromatin activation (histone H3 lysine 27 acetylation (H3K27Ac) and histone H3 lysine 4 trimethylation (H3K4me3)) and repression (histone H3 lysine 27 trimethylation (H3K27me3)). To differentiate endogenous *MLL1/KMT2A* from *MLL-AF9*, we used an approach employing antibodies binding either the N- or C-terminus of *MLL1/KMT2A* [23]. Differentiation of binding by the fusion oncoprotein from endogenous *MLL1/KMT2A* as a function of the cell of origin is a crucial consideration since *MLL1/KMT2A* is a key regulator of normal HSC self-renewal, and normal HSC self-renewal programs maintained by *MLL1/KMT2A* and aberrant self-renewal programs driven by *MLL-AF9* may overlap [24]. This strategy therefore allows us to deduce inherited programs independent of the oncoprotein (both *MLL1/KMT2A* N- and C-bound) and those driven by the fusion oncoprotein (predominantly N-bound) as a function of the epigenetic state of the cell of origin.

As expected, we found that the binding profiles of the *MLL-N* and *MLL-C* antibodies showed partial overlap by cell of origin, with patterns of binding specific to each cell of origin and many binding sites shared between leukemias from each cell of origin (Fig. 3A, B). We first focused on loci bound by *MLL-AF9* specifically (marked by only the *MLL-N* antibody). We found that while there were many peaks shared by each AML, MPP- and Prog-AMLS had the highest number of unique N-specific/*MLL-AF9*-bound peaks identified as significantly enriched compared to HSC-AML (Figs. 3C, D, S3A, Table S3). This suggested that the *MLL-AF9* oncoprotein was binding key oncogenic loci in MPPs and progenitors that may have been already active in HSCs to ectopically confer LSC-like programs in non-stem cells. Indeed, we observed that the *MLL-N* antibody showed stronger binding to the loci encoding the key AML transcription factors (TFs) *MEIS1*, *PBX3*, *MEF2C*, *MYB*, *RUNX2*, and the *HOXA* cluster in MPP- and Prog-AMLS compared to HSC-AML (Fig. 3E, S3B-D) [25–27]. However, all AMLs showed similar patterns of H3K27Ac, H3K4me3 and H3K27me3 at these loci, consistent with equal degrees of overall activation (Fig. 3E, S3B-D). These results suggest that expression of these TFs is maintained relatively independently of *MLL-AF9* in HSC-AML – with their activated chromatin status inherited from the HSC of origin – while MPP- and Prog-AML depend on the *MLL-AF9* oncoprotein to drive their expression for participation in LSC self-renewal pathways. Interestingly, we observed that *MLL-AF9* could not access the *MECOM* locus in Prog-AML as this locus is associated with high H3K27me3 binding; and while there was a high degree of *MLL-AF9* binding at *MECOM* in MPP-AML, this was lower in HSC-AML (Figs. S3E, S4A). This indicates that *MECOM* is sufficiently silenced in normal progenitors to preclude ectopic activation by *MLL-AF9*, while this stem cell TF is ectopically activated by *MLL-AF9* in MPP-AML, and its activated state is inherited from the HSC of origin in HSC-AML. By comparing the loci bound by *MLL-AF9* specifically (i.e., N-only bound peaks) in MPP-AML or Prog-AML to

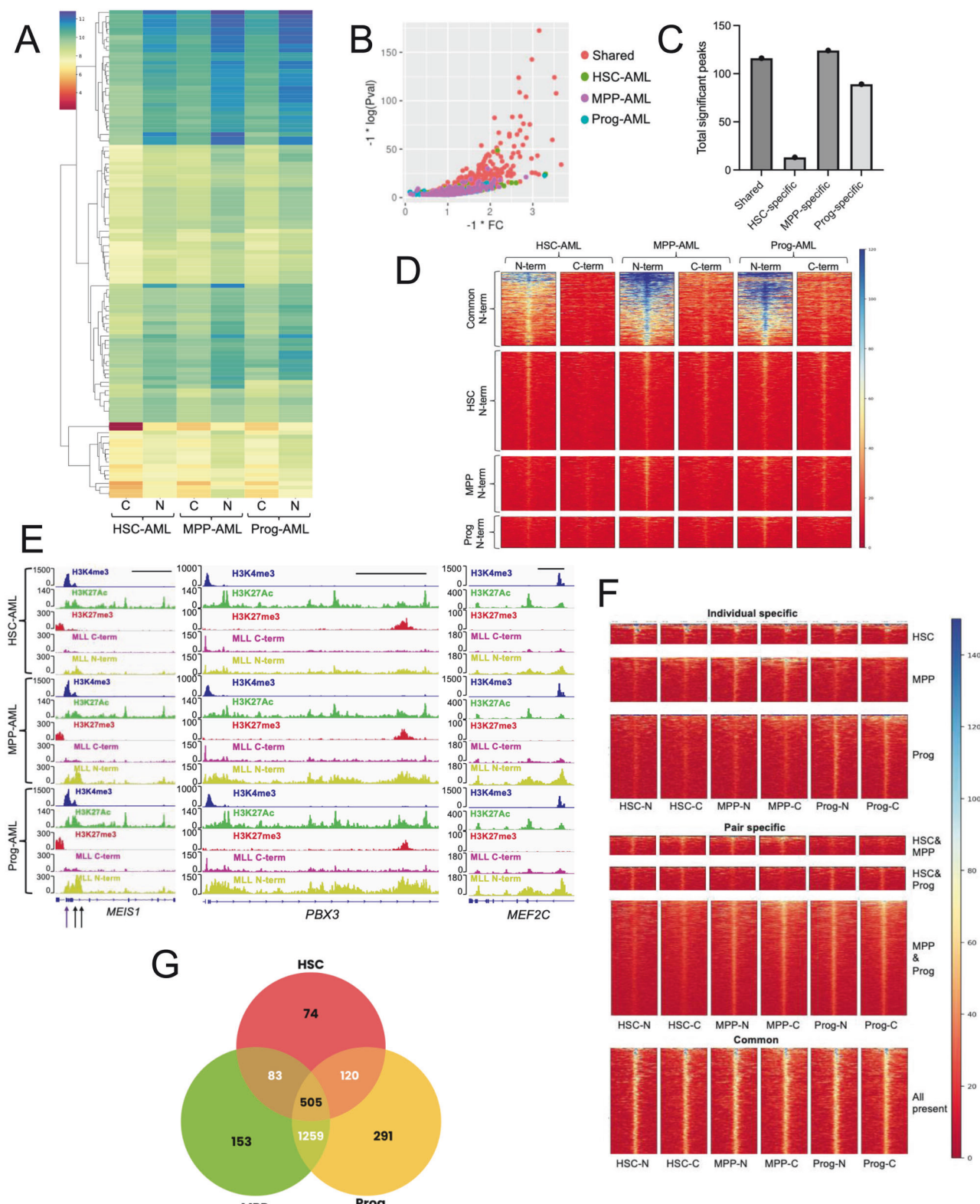
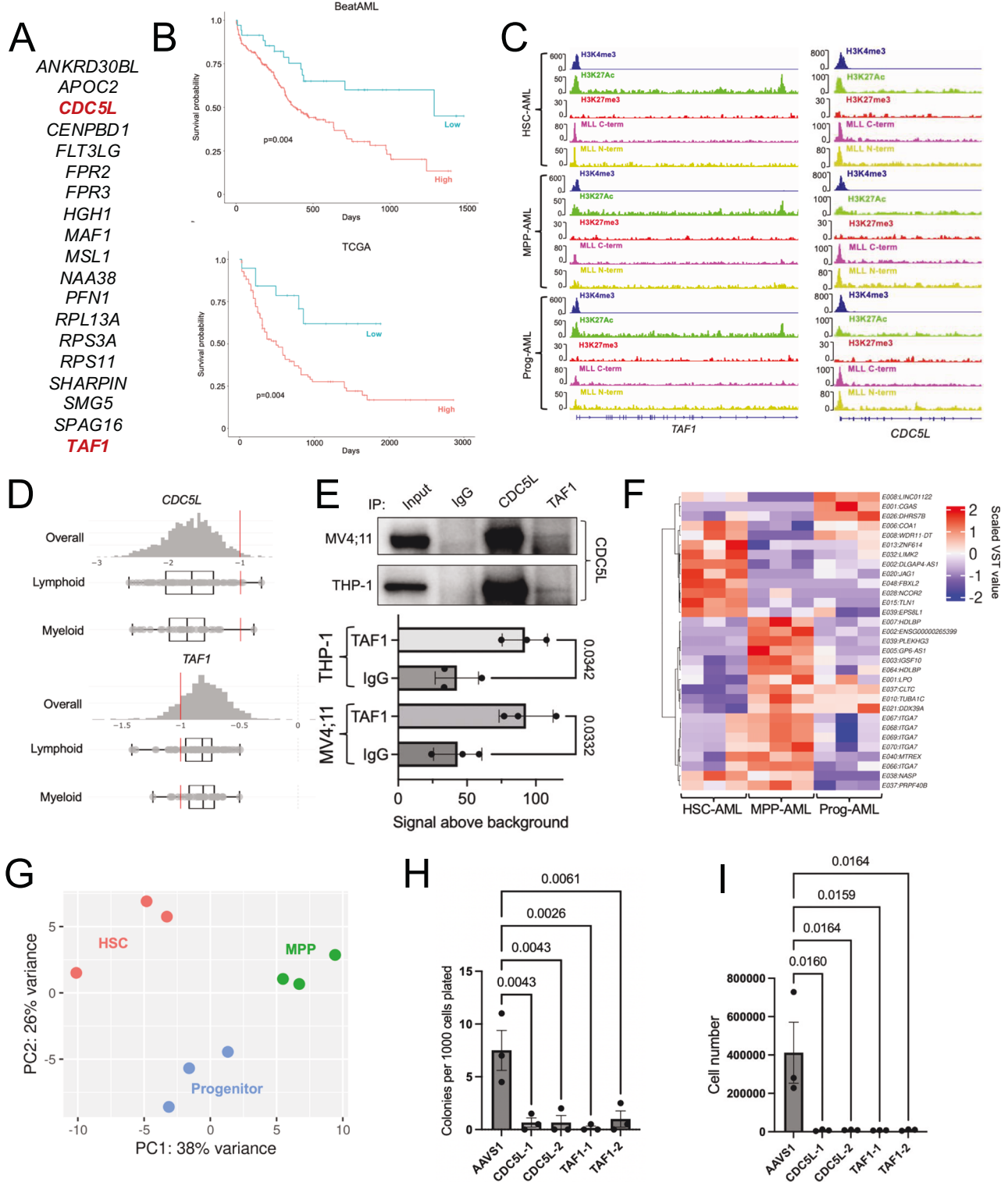


Fig. 3 Defining the global MLL-AF9-driven and -independent epigenome of AMLs of defined cellular origin. **A** Heatmap showing peaks and associated genes bound by MLL-N or MLL-C for AMLs of defined origins. Scatterplot **B** and total number of significant MLL-N-specific peaks **C** from AMLs of the indicated origins. **D** Tornado plots showing MLL-N peaks in the indicated cell states/categories. **E** Representative CUT&RUN tracks at the indicated loci for the indicated chromatin binding proteins. **F** Tornado plots showing shared co-bound MLL-N/C peaks for the indicated AMLs/categories. **G** Venn diagram showing the numbers of shared and cell of origin-specific double bound MLL-N/C peaks.



transcriptional profiles of healthy defined HSPC populations, we did not observe that these epigenetic signatures aligned with the HSC transcriptome, indicating that they were not implementing normal HSC programs, rather ectopic programs containing select multipotency TFs (Fig. S5A, B, Table S4) [21]. Together, these data indicate that the MLL-AF9 fusion oncprotein differentially impacts AMLs as a function of the epigenetic milieu of the HSPC of origin.

Epigenetic effects of MLL1/KMT2A in inheritance from the cell of origin

Next, with the objective of defining programs that distinguish HSC-AML independently of the MLL-AF9 oncogene, we examined loci occupied by both MLL-N and MLL-C antibodies to define endogenous MLL1/KMT2A-bound loci. In the three types of AML, we observed shared and cell-of-origin specific programs that were more reflective of the transcriptional programs of cognate normal

Fig. 4 AML dependencies identified in the HSC-AML epigenetic program. **A** Candidate HSC-AML inherited epigenetic program. **B** Calculation of HSC-AML epigenetic signature using the BeatAML dataset (*CDC5L* + *PFN1* + *SMG5* + *TAF1* + *SHARPIN* + *FLT3LG* + *SPAG16* + *FPR2* + *FPR3*) with the significance threshold identified in the BeatAML dataset independently validated in The Cancer Genome Atlas (TCGA) AML dataset. Kaplan-Meier survival curves are shown with *p* values calculated by log rank test. **C** CUT&RUN tracks at the indicated loci for the indicated chromatin-bound proteins. **D** Broad Dependency Map output for lymphoid and myeloid leukemia cell lines for *CDC5L* and *TAF1*. **E** Co-immunoprecipitation and western blotting for the indicated proteins. Graph shows quantification of *CDC5L* western signal for IgG or *TAF1* immunoprecipitation above background (*n* = 3 independent experiments compared by one-way ANOVA with *p*-values shown). **F** RNA sequencing analysis of differentially utilized exons (in some cases multiple exons per gene) among the indicated AMLs (scaled VST value shown). **G** PCA of AML transcriptomes based on exon usage. **H** HSC-AML were transduced with lentiviruses encoding Cas9 and the indicated gRNAs and placed in CFU assays. Colony formation was scored after 10–14 days (*n* = 3 independent experiments, results compared by ANOVA with *p* values shown). **I** MV4;11 cells were transduced with lentiviruses encoding Cas9 and the indicated gRNAs and 20,000 cells were plated in culture to monitor growth. Six days later, cell growth was quantified (*n* = 3 independent experiments, results compared by ANOVA with *p* values shown).

HSPC populations than MLL-AF9 driven programs (Fig. 3F–G, Fig. S5C, D, Tables S4 and S5) [21]. Notably, we identified an endogenous MLL1-bound program specific to HSC-AML, suggesting inheritance from the cell of origin (Fig. 3F–G). We curated this HSC-AML-specific program to focus on genes expressed in the hematopoietic system with defined functions and visually validated peak specificity to narrow candidate loci putatively inherited from the HSC of origin to HSC-AML (Fig. 4A). We used this program to devise a putative HSC-AML epigenetic signature score that associated with poor outcome in a discovery AML patient dataset (BeatAML) that we then validated in the independent AML dataset (TCGA; Fig. 4B) [28]. In a multivariate regression analysis, this signature was a significant factor in predicting prognosis independently of all co-variables tested except *DNMT3A* and *TP53* mutation status (likely due to low power for these parameters); notably, the signature score was significantly prognostic independently of *MLL* translocation status (Fig. S6).

Given the vital role of transcriptional activation, elongation, and splicing in AML and leukemias driven by *MLL1/KMT2A* translocations, we focused on the putative program components *TAF1* – encoding a component of the TFIID transcriptional initiation complex, and *CDC5L*, encoding a component of the PRP19 splicing machinery (Fig. 4C) [29–31]. *TAF1* and *CDC5L* are dependencies in myeloid and lymphoid acute leukemia cell lines and are physically complexed in *MLL*-rearranged AML cells (Fig. 4D, E) [32]. Expression of *TAF1* and *CDC5L* is enriched in healthy HSCs, with higher chromatin accessibility at these loci compared to more differentiated HSPCs (Fig. S4B, C). Moreover, in our dataset, we observed differential patterns of exon inclusion/exclusion as a function of the cell of origin, consistent with variable mRNA splicing (Fig. 4F, G, Table S6). Based on these data, we used CRISPR to delete *TAF1* or *CDC5L* in HSC-AML and an *MLL*-rearranged AML cell line, confirming these genes as dependencies for clonogenesis and growth (Fig. 4H, I). Together, these findings implicate a program of transcriptional initiation and differential splicing as inherited from the cell of origin in AML with potential impact on AML biology.

RNAP II transcription as a vulnerability in HSC AML

To better the roles of RNA synthesis in AMLs of defined origin, we performed CUT&RUN for RNA polymerase II (RNAPII). Early post-transformation, we found that AMLs of multipotent origin showed more RNAP II-bound loci compared to Prog-AML, suggestive of a higher degree of RNAP II recruitment (Fig. 5A). Consistent with a role for RNAP II binding in AML driven by *MLL* translocations, *MLL*-rearranged cell lines showed increased sensitivity to RNAP II inhibition with either actinomycin D (stabilizer of DNA double helix to prevent transcriptional initiation by RNAP) or α-amanitin (inhibitor of RNAP II translocation) compared to a non-*MLL*-rearranged line (Fig. 5B, C). In contrast to the relative resistance of HSC-AML to agents used in induction chemotherapy (Fig. 2E), HSC-AML did not show the same degree of resistance

to actinomycin D relative to MPP- and Prog-AML in viability assays, while also showing a greater relative diminishment of clonogenesis in LT-IC and colony formation assays compared to MPP- and Prog-AML (HSC-AML 85%, MPP-AML 74%, Prog-AML 63% average reduction in colony formation assays; fold changes in LT-ICs shown; Fig. 5D–F). Finally, upon xenotransplantation, we found that growth and survival of HSC-AML *in vivo* was markedly impaired by actinomycin D treatment (Fig. 5G). Overall, these findings demonstrate a sensitivity of HSC-AML cells to inhibition of RNAP II relative to standard induction chemotherapy agents.

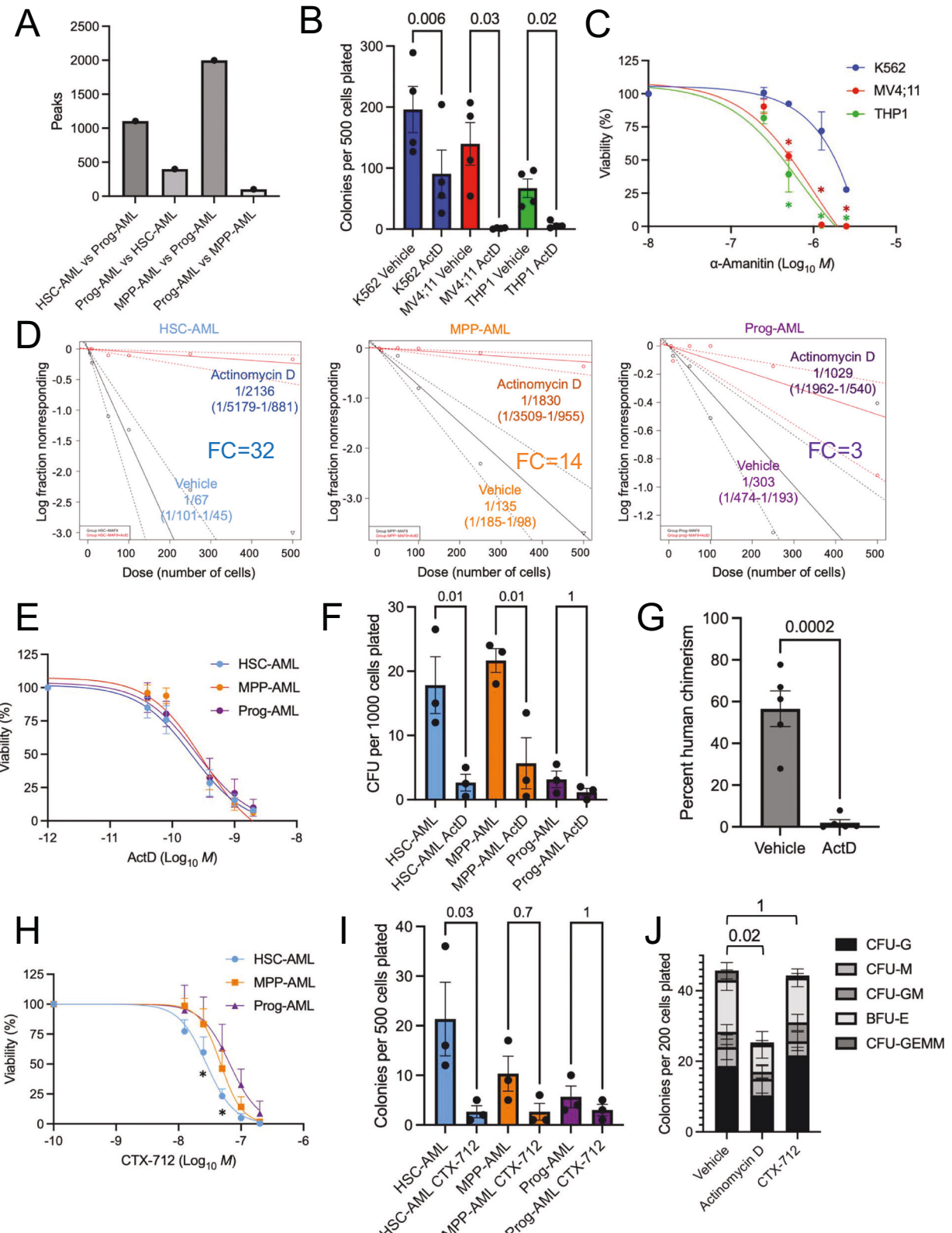
Therapeutically targeting splicing factor aberrations is a major area of focus in AML [33, 34]. To test sensitivity of AMLs to perturbation of splicing, we used CTX-712, an inhibitor of CLK family kinases that phosphorylate the serine-rich domains of splicing factors to regulate splicing [35]. We found that HSC-AML showed sensitivity to CTX-712 to a greater degree than MPP- and Prog-AML in viability and colony formation assays (percent decrease in colony formation – HSC AML 87%, MPP-AML 77%, Prog-AML 47%; Fig. 5H, I). Notably, untransformed human HSPCs showed lower overall sensitivity to actinomycin D and CTX-712 compared to AMLs (Fig. 5J).

DISCUSSION

Here, we show that in a human setting using an endogenously regulated oncogene, AML of HSC origin most persistently sustains stem cell activity. Using epigenomic profiling, we observe context-dependent effects of the action of the MLL-AF9 oncprotein as well as inherited epigenetic programs dependent on the cell of origin. A portion of this program includes RNAP II recruitment via *TAF1*/TFIID and mRNA splicing, a key pathway often perturbed in leukemia [36, 37].

The notion that the normal cell of origin can impact the behavior of leukemia has been previously investigated in several mouse- and human-based models. Within the mature adult hematopoietic ontogeny, ectopic retroviral overexpression of *MLL*-AF9 in mouse HSCs resulted in more aggressive leukemia compared to myeloid progenitors with evidence of a distinct HSC-driven gene expression program [5]. In mouse models, it was reported that the signature of the cell of origin could be detected based on chromatin accessibility [9]. On a mechanistic level, in humans, lentiviral-mediated overexpression of *MLL* fusion oncogenes resulted in more aggressive AML derived from HSCs compared to progenitors and resistance to standard chemotherapy attributed to expression of xenobiotic efflux transporters [38]. Our findings extend these results by demonstrating that endogenously regulated expression by CRISPR/Cas9 engineering of the *MLL*-AF9 oncogene in defined HSPCs of origin differentially impacts leukemia behavior.

At early time points post transformation, we observed similar behavior of leukemias regardless of origin. In the medium-term, HSC and MPP leukemias maintained LSC functionality, while in the



long-term, only HSC leukemia maintained robust LSC self-renewal. In a previous human study, distinctions were not clearly made between multipotent HSC and MPP cells of origin in terms of leukemic behavior or stem cell properties, but in mice, AML of HSC and MPP origin seemed to be more aggressive compared to that

from myeloid progenitors [9, 38]. Although we identify an HSC-specific epigenetic program and HSC leukemia shows the most durable maintenance of LSC function, our transcriptomic profiling indicates that there is graded maintenance of LSC properties along the spectrum of multipotent to more lineage-restricted

Fig. 5 Vulnerability of HSC AML to transcriptional inhibition and perturbation of mRNA splicing. **A** CUT&RUN for RNAP II was performed on AMLs of each HSPC origin at day 44 post transformation, and significant peak enrichment by MACS2 for the indicated comparisons is shown. **B** The indicated cell lines were pretreated with actinomycin D (ActD, 5 nM) for 6 h and then placed in colony formation assays. Ten days later, colony formation was blindly scored ($n = 4$ independent experiments, * $p < 0.05$ for the indicated comparisons by paired student's *t*-test). **C** The indicated cell lines were cultured with varying concentrations of α -amanitin for 4 days at which time viability was measured ($n = 3$ independent experiments, * $p < 0.01$ for MV4;11 (red) and THP-1 (green) compared to K562 by student's *t*-test). **D** LT-IC assays in which the indicated AMLs were plated at variable cell doses in the presence or absence of 1 nM actinomycin D for 4 days, at which time the drug was washed out. After three weeks, clonal outgrowths were blindly scored (results pooled from $n = 2$ independent experiments from independent donors/initial cultures; p values for vehicle versus actinomycin D by limiting dilution analysis: HSC: 4×10^{-21} , MPP 3×10^{-15} , Prog 0.001). Fold changes (FC) between vehicle and actinomycin D are shown. **E** The indicated AMLs were cultured with varying concentrations of actinomycin D for 4 days at which time viability was measured ($n = 3$ independent experiments, $p = \text{NS}$ for all comparisons). **F** The indicated AMLs were pretreated with actinomycin D (ActD, 5 nM) for 6 h and then placed in colony formation assays. Fourteen days later, colony formation was blindly scored ($n = 3$ independent experiments, p values shown by one-way ANOVA). **G** HSC-AML was xenotransplanted intrafemorally into NSG mice. Mice were then treated with actinomycin D for two weeks, after which time chimerism was analyzed (p value shown by unpaired student's *t*-test). **H** The indicated AMLs lines were cultured with varying concentrations of CTX-712 for 4 days at which time viability was measured ($n = 3$ independent experiments, * $p < 0.01$ for MPP-AML and Prog-AML compared to HSC-AML by student's *t*-test). **I** The indicated AMLs were pretreated with CTX-712 (3 uM) for 6 h and then placed in colony formation assays. Fourteen days later, colony formation was blindly scored ($n = 3$ independent experiments, p values shown by one-way ANOVA). **J** Human CD34⁺ HSPCs were pretreated with either vehicle, actinomycin D (5 nM) or CTX-712 (3 uM) for 6 h and then placed in colony formation assays. Fourteen days later, colony formation was blindly scored ($n = 3$ independent donors, p values of total colony counts compared by one-way ANOVA and shown). In all panels, results are presented as mean \pm SEM.

HSPCs. Future work will focus on understanding these mechanisms of exhaustion of LSCs in non-HSC AML.

We observed effects of the cell of origin both on programs directly passed to leukemia as well as on action of the MLL-AF9 oncogene. MLL-AF9 showed varying effects on binding target loci that are impacted by the epigenetic state of the cell of origin. Although AMLs of each cell of origin showed similar histone profiles at the *MEIS1*, *PBX3*, and *MEF2C* loci that encode key AML TFs, there were varying degrees of MLL-AF9 binding at these loci marked by the N-terminal antibody specifically, with more MLL-AF9 binding in MPP and progenitor AML. This indicates that these loci are ectopically activated in MPP- and Prog-AML to confer LSC-like self-renewal, at least temporarily, while the epigenetic state of HSC-AML appears to render this unnecessary, requiring less overall activity of the fusion to implement and maintain LSC programs. Although these AMLs are initiated from HSPCs with variable self-renewal, the action of the MLL-AF9 oncogene elevates the self-renewal potential of MPPs and progenitors in the short-term to that of HSCs but does not impact long-term maintenance of LSCs. Our approach of epigenetic profiling and analysis of fusion oncogene binding reveals dual effects of the cell of origin in programming the downstream AML – the epigenetic milieu of the HSPC of origin defines the target loci and actions of the fusion oncogene to define ectopic oncogene-driven programs, and inheritance of oncogene-independent programs can additionally confer growth and survival dependencies. While we demonstrate these effects in the experimentally tractable MLL-AF9 system – which is a potent oncogene sufficient to initiate transformation autonomously in experimental models – we speculate that this paradigm holds in the case of other fusion oncogene drivers.

To better understand the aggressiveness of HSC-AML, we focused on loci with cell of origin-specific chromatin states independent of MLL-AF9 binding. These loci were associated with varying profiles of chromatin activation that aligned with binding of full-length endogenous MLL1/KMT2A, a vital self-renewal factor in normal HSCs [24]. This is consistent with an epigenetically inherited program that is unaffected by the MLL-AF9 oncogene, specific to the cell of origin, and potentially at least partially responsible for differences in maintenance of LSC self-renewal. This program was diverse in its composition, including *APOC2*, the expression of which is associated with poor prognosis and activates cell proliferation via *CD36*, *FLT3LG*, which plays a key role in AML blast proliferation, *FPR2/3*, which act as proinflammatory/chemotactic factors, and genes with unclear function in hematopoiesis (*ANKRD30BL*, *CENPBD1*, *SPAG16*) [39–41]. Using these loci, while we devised an HSC-AML signature score that appears

to have prognostic significance, further characterization of primary patient AML specimens is required to validate an association of this signature with a bona fide HSC cell of origin through the use of additional biomarkers. Prospective validation of this HSC-AML signature in further independent AML datasets is warranted prior to consideration of clinical implementation.

Interestingly, the inherited HSC-AML program contained elements of globally important cellular functions, including transcription (*TAF1*), mRNA splicing (*CDC5L*), protein chaperone function (*HGH1*), tRNA biogenesis (*MAF1*), cytoskeletal function (*PFN1*), protein degradation (*SHARPIN*), RNA stability (*SMG5*), genome integrity (*MSL1*), and translation (*RPL13A*, *RPS3A*, *RPS11*), suggesting that HSC-AML bears heightened dependency on these processes for implementation of stem cell programs [42]. Informed by biology of MLL fusions and AML oncogenesis, we validated dependency of HSC-AML on *TAF1* and *CDC5L* in HSC-AML. The dependency of HSC-AML on transcriptional initiation and splicing could be exploited by pharmacologic treatment with actinomycin D, an inhibitor of RNAP II binding to DNA, or CTX-712, an inhibitor of CLK kinases. Although AML of all origins were sensitive to both compounds, HSC-AML tended to show a stronger fold-decrease in colony formation, suggestive of mitigation of the elevated stem cell content relative to MPP-AML and Prog-AML. These results align with recent work advancing actinomycin D as a candidate therapy in NPM1c-mutant AML, and our results using normal human HSPCs suggest a therapeutic index for both compounds [43].

Overall, we show that the HSPC of origin impacts the LSC behavior of AML due to differential effects of the MLL-AF9 oncogene imposed on the epigenetic state of the cell of origin, and that elements of the HSPC epigenome are likely inherited by AML to define its behavior. While our findings are most likely immediately relevant to pediatric AML in that we used juvenile HSPCs of origin, since age of the hematopoietic system impacts manifestations of leukemia, further validation in AMLs across the age spectrum is warranted [14, 44, 45]. We observe that AMLs show heightened sensitivity to inhibition of transcriptional initiation and splicing compared to normal human HSPCs, possibly due to a requirement for these pathways in transformation by the MLL-AF9 oncogene. These findings form a basis for future epigenomic profiling of AMLs to further refine risk stratified treatment schema based on cell of origin signatures.

METHODS

All studies were performed in accordance with the relevant guidelines and regulations.

HSPC isolation and gene editing

Usage of human specimens was approved by the Institutional Review Board of Boston Children's Hospital. Informed consent was obtained from all subjects. Human cord blood CD34⁺ HSPCs (Stem Cell Tech) were cultured X-VIVO-15 medium (Lonza) with 1% BSA fraction V (Gibco) and human stem cell cytokines (SCF 100 ng/ml, FLT3L 100 ng/ml and TPO 50 ng/ml, Peprotech) for 24 h. 300 pmol modified synthetic sgRNAs (Synthego, Table S7) were complexed with 60 pmol of purified Cas9 Nuclease (Integrated DNA Technologies) for 15 min at room temperature. 200,000 HSPCs were washed with PBS twice and mixed with the ribonucleoprotein (RNP) complex in a total of 20ul Nucleofector Solution (Lonza). The mixture was transferred into the 16-well Nucleocuvette Strips and electroporated with a 4D Nucleofector with program EO-100 (Lonza). Twenty-four hours later, HSPCs were washed and stained with antibodies (CD34, CD38, CD45RA, CD90, and Lineage cocktail, Table S8) and defined HSPC populations were sorted on a FACS ARIA II Cytometer (BD Biosciences). Sorted cells were maintained in pro-myeloid culture conditions for monitoring of growth and transformation (IMDM supplemented with 20% FBS and SCF 100 ng/ml, FLT3L 100 ng/ml, TPO 50 ng/ml, IL-3 10 ng/ml, and IL-6 100 ng/ml). A fraction of HSPCs was harvested 15 days post electroporation for analysis of editing. Genomic DNA was extracted using the QuickExtract DNA Extraction Solution (Lucigen) and PCR was performed to validate the presence of *MLL-AF9* fusion (Table S9).

CUT & RUN

Edited HSPC populations cultured for 39 days and transformed to AML were harvested and subjected to CUT&RUN assay following the manufacturer's protocol (EpiCypher). Briefly, 500,000 cells were spun and washed twice with wash buffer (20 mM HEPES pH 7.5, 150 mM NaCl, 0.5 mM spermidine, Roche Complete Protease Inhibitor EDTA-Free). Samples were then bound to activated ConA beads, resuspended in antibody buffer (wash buffer containing 0.01% digitonin and 2 mM EDTA) and incubated with primary antibody on a nutator at 4 °C overnight. On the second day, samples were washed and incubated with secondary antibody in wash buffer at 4 °C for 1 h. Samples were subsequently washed twice with cold cell permeabilization buffer (wash buffer containing 0.01% digitonin) and incubated with pAG-MNase for 10 min at room temperature. After two washes with cell permeabilization buffer, samples were processing to fragmentation by incubating with 2 mM Calcium Chloride at 4 °C for 2 h. Then, Stop Buffer Master Mix was added to each reaction and samples were incubated on a block heater at 37 °C for 30 min for fragmented DNA release. The DNA was then extracted using the phenol-chloroform-isoamyl alcohol (Sigma) method in phase-lock tubes (Qiagen MaXtract). The purified DNA was either stored at -20 °C or further processed to library preparation using the NEBNext Ultra II DNA Library Prep Kit for Illumina (NEB). Libraries were cleaned with a single round of AMPure XP beads (Beckman Colter) at a 1.2 to 1 (vol/vol) ratio of beads to sample. Library concentration was checked by Qubit fluorometer (Thermo Fisher) and library size distribution was evaluated on a TapeStation Bioanalyzer instrument (Agilent). Sequencing was done at the Molecular Biology Core Facility at the Dana-Farber Cancer Institute.

Xenotransplantation

All animal experiments were approved by the Institutional Care and Use Committee at Boston Children's Hospital. 1-2 x 10⁶ cultured CRISPR/Cas9-edited HSC, MPP or progenitor cells were intravenously transplanted into sublethally irradiated (275 cGy) NSG (NOD.Cg-*Prkdc*^{scid} *Il2rg*^{tm1Wjl}/SzJ) female mice (Jackson Laboratory). Antibiotics were added to the drinking water for one month after irradiation. In some experiments, human engraftment and disease progression were monitored by flow cytometric analysis of human CD45+ cells in peripheral blood every 4 weeks. Mice were humanely euthanized when experimental endpoints consistent with systemic symptoms of leukemia based on weight loss and body condition score were reached. For all animal studies, power calculations were performed to detect a

30% difference in survival with expected standard deviation of 10% and an alpha cutoff of 0.05.

Cell culture

Human AML cell lines MV4;11 and THP-1 were purchased from ATCC and were maintained in IMDM supplemented with 20% FBS. HEK-293 cells were obtained from ATCC and cultured in DMEM with 10% FBS for lentivirus production. All cell lines were used at low passage following authentication. Routine Mycoplasma testing was performed every two weeks.

DATA AVAILABILITY

Sequencing data are available in Gene Expression Omnibus (GSE262561).

REFERENCES

1. Gardon N, Marchi E, Atzberger A, Quek L, Schuh A, Soneji S, et al. Coexistence of LMPP-like and GMP-like leukemia stem cells in acute myeloid leukemia. *Cancer Cell*. 2011;19:138–52.
2. le Viseur C, Hotfilder M, Bomken S, Wilson K, Rottgers S, Schrauder A, et al. In childhood acute lymphoblastic leukemia, blasts at different stages of immunophenotypic maturation have stem cell properties. *Cancer Cell*. 2008;14:47–58.
3. Sarry JE, Murphy K, Perry R, Sanchez PV, Secretro A, Keefer C, et al. Human acute myelogenous leukemia stem cells are rare and heterogeneous when assayed in NOD/SCID/IL2Rgamma-mac-deficient mice. *J Clin Invest*. 2011;121:384–95.
4. Eppert K, Takenaka K, Lechman ER, Waldron L, Nilsson B, van Galen P, et al. Stem cell gene expression programs influence clinical outcome in human leukemia. *Nat Med*. 2011;17:1086–93.
5. Krivtsov AV, Figueroa ME, Sinha AU, Stubbs MC, Feng Z, Valk PJ, et al. Cell of origin determines clinically relevant subtypes of MLL-rearranged AML. *Leukemia*. 2013;27:852–60.
6. Ng SW, Mitchell A, Kennedy JA, Chen WC, McLeod J, Ibrahimova N, et al. A 17-gene stemness score for rapid determination of risk in acute leukaemia. *Nature*. 2016;540:433–7.
7. Wahlster L, Daley GQ. Progress towards generation of human hematopoietic stem cells. *Nat Cell Biol*. 2016;18:1111–7.
8. Buenrostro JD, Corces MR, Lareau CA, Wu B, Schep AN, Aryee MJ, et al. Integrated single-cell analysis maps the continuous regulatory landscape of human hematopoietic differentiation. *Cell*. 2018;173:1535–1548.e1516.
9. George J, Uyar A, Young K, Kufller L, Waldron-Francis K, Marquez E, et al. Leukaemia cell of origin identified by chromatin landscape of bulk tumour cells. *Nat Commun*. 2016;7:71266.
10. Zeisig BB, Garcia-Cuellar MP, Winkler TH, Slany RK. The oncogene MLL-ENL disturbs hematopoietic lineage determination and transforms a biphenotypic lymphoid/myeloid cell. *Oncogene*. 2003;22:1629–37.
11. Pei S, Minhajuddin M, Adane B, Khan N, Stevens BM, Mack SC, et al. AMPK/FIS1-mediated mitophagy is required for self-renewal of human AML stem cells. *Cell Stem Cell*. 2018;23:86–100.e106.
12. Kreso A, Dick JE. Evolution of the cancer stem cell model. *Cell Stem Cell*. 2014;14:275–91.
13. Wang JC, Dick JE. Cancer stem cells: lessons from leukemia. *Trends Cell Biol*. 2005;15:494–501.
14. Rowe RG, Lumertz da Rocha E, Sousa P, Missios P, Morse M, Marion W, et al. The developmental stage of the hematopoietic niche regulates lineage in MLL-rearranged leukemia. *J Exp Med*. 2019;216:527–38.
15. Morris V, Wang D, Li Z, Marion W, Hughes T, Sousa P, et al. Hypoxic, glycolytic metabolism is a vulnerability of B-acute lymphoblastic leukemia-initiating cells. *Cell Rep*. 2022;39:110752.
16. Polley DA, Jordan CT. Therapeutic targeting of acute myeloid leukemia stem cells. *Blood*. 2017;129:1627–35.
17. Jeong J, Jager A, Domizi P, Pavel-Dinu M, Gojenola L, Iwasaki M, et al. High-efficiency CRISPR induction of t(9;11) chromosomal translocations and acute leukemias in human blood stem cells. *Blood Adv*. 2019;3:2825–35.
18. Doulatov S, Notta F, Laurenti E, Dick JE. Hematopoiesis: a human perspective. *Cell Stem Cell*. 2012;10:120–36.
19. Cesana M, Guo MH, Cacchiarelli D, Wahlster L, Barragan J, Doulatov S, et al. A CLK3-HMGA2 alternative splicing axis impacts human hematopoietic stem cell molecular identity throughout development. *Cell Stem Cell*. 2018;22:575–588.e577.
20. Liu Z, Gu Y, Chakarov S, Bleriot C, Kwok I, Chen X, et al. Fate mapping via Ms4a3-expression history traces monocyte-derived cells. *Cell*. 2019;178:1509–1525.e1519.
21. Aguade-Gorgorio J, Jami-Alahmadi Y, Calvanese V, Kardouh M, Fares I, Johnson H, et al. MYCT1 controls environmental sensing in human hematopoietic stem cells. *Nature*. 2024;630:412–20.

22. Skene PJ, Henikoff S. An efficient targeted nuclease strategy for high-resolution mapping of DNA binding sites. *Elife*. 2017;6:e21856.
23. Janssens DH, Meers MP, Wu SJ, Babaeva E, Meshinchic S, Sarthy JF, et al. Automated CUT&Tag profiling of chromatin heterogeneity in mixed-lineage leukemia. *Nat Genet*. 2021;53:1586–96.
24. Jude CD, Climer L, Xu D, Artinger E, Fisher JK, Ernst P. Unique and independent roles for MLL in adult hematopoietic stem cells and progenitors. *Cell Stem Cell*. 2007;1:324–37.
25. Guo H, Chu Y, Wang L, Chen X, Chen Y, Cheng H, et al. PBX3 is essential for leukemia stem cell maintenance in MLL-rearranged leukemia. *Int J Cancer*. 2017;141:324–35.
26. Kumar AR, Li Q, Hudson WA, Chen W, Sam T, Yao Q, et al. A role for MEIS1 in MLL-fusion gene leukemia. *Blood*. 2009;113:1756–8.
27. Tarumoto Y, Lu B, Somerville TDD, Huang YH, Milazzo JP, Wu XS, et al. LKB1, salt-inducible kinases, and MEF2C are linked dependencies in acute myeloid leukemia. *Mol Cell*. 2018;69:1017–1027.e1016.
28. Tyner JW, Tognon CE, Bottomly D, Wilmot B, Kurtz SE, Savage SL, et al. Functional genomic landscape of acute myeloid leukaemia. *Nature*. 2018;562:526–31.
29. Bewersdorf JP, Abdel-Wahab O. Translating recent advances in the pathogenesis of acute myeloid leukemia to the clinic. *Genes Dev*. 2022;36:259–77.
30. Yokoyama A. Transcriptional activation by MLL fusion proteins in leukemogenesis. *Exp Hematol*. 2017;46:21–30.
31. Smith E, Lin C, Shilatifard A. The super elongation complex (SEC) and MLL in development and disease. *Genes Dev*. 2011;25:661–72.
32. Tsherniak A, Vazquez F, Montgomery PG, Weir BA, Kryukov G, Cowley GS, et al. Defining a cancer dependency map. *Cell*. 2017;170:564–576.e516.
33. Figg JW, Barajas JM, Obeng EA. Therapeutic approaches targeting splicing factor mutations in myelodysplastic syndromes and acute myeloid leukemia. *Curr Opin Hematol*. 2021;28:73–79.
34. Lee SC, Dvinge H, Kim E, Cho H, Micl JB, Chung YR, et al. Modulation of splicing catalysis for therapeutic targeting of leukemia with mutations in genes encoding spliceosomal proteins. *Nat Med*. 2016;22:672–8.
35. Araki S, Dairiki R, Nakayama Y, Murai A, Miyashita R, Iwatani M, et al. Inhibitors of CLK protein kinases suppress cell growth and induce apoptosis by modulating pre-mRNA splicing. *PLoS ONE*. 2015;10:e0116929.
36. Dvinge H, Kim E, Abdel-Wahab O, Bradley RK. RNA splicing factors as oncogenes and tumour suppressors. *Nat Rev Cancer*. 2016;16:413–30.
37. Yoshimi A, Lin KT, Wiseman DH, Rahman MA, Pastore A, Wang B, et al. Coordinated alterations in RNA splicing and epigenetic regulation drive leukaemogenesis. *Nature*. 2019;574:273–7.
38. Zeisig BB, Fung TK, Zarowiecki M, Tsai CT, Luo H, Stanojevic B, et al. Functional reconstruction of human AML reveals stem cell origin and vulnerability of treatment-resistant MLL-rearranged leukemia. *Sci Transl Med*. 2021;13:eabc4822.
39. Zhang T, Yang J, Vaikari VP, Beckford JS, Wu S, Akhtari M, et al. Apolipoprotein C2 - CD36 promotes leukemia growth and presents a targetable axis in acute myeloid leukemia. *Blood Cancer Discov*. 2020;1:198–213.
40. Leung AY, Man CH, Kwong YL. FLT3 inhibition: a moving and evolving target in acute myeloid leukaemia. *Leukemia*. 2013;27:260–8.
41. Weiss E, Kretschmer D. Formyl-peptide receptors in infection, inflammation, and cancer. *Trends Immunol*. 2018;39:815–29.
42. Agudo-Llera D, Hamidi T, Domenech R, Pantoja-Uceda D, Gironella M, Santoro J, et al. Deciphering the binding between Nupr1 and MSL1 and their DNA-repairing activity. *PLoS ONE*. 2013;8:e78101.
43. Wu HC, Rerolle D, Berthier C, Hleihel R, Sakamoto T, Quentin S, et al. Actinomycin D TARGETs NPM1c-primed mitochondria to restore PML-driven senescence in AML therapy. *Cancer Discov*. 2021;11:3198–213.
44. Man N, Sun XJ, Tan Y, Garcia-Cao M, Liu F, Cheng G, et al. Differential role of Id1 in MLL-AF9-driven leukemia based on cell of origin. *Blood*. 2016;127:2322–6.
45. Jassinskaia M, Ghosh S, Watral J, Davoudi M, Claesson Stern M, Daher U, et al. A complex interplay of intra- and extracellular factors regulates the outcome of fetal- and adult-derived MLL-rearranged leukemia. *Leukemia*. 2024;38:1115–30.

ACKNOWLEDGEMENTS

This work was supported by the V Foundation, the National Institute for Diabetes, Digestive, and Kidney Disorders (R01DK134515), the Department of Defense (W81XWH2110301 and Convergent Science Virtual Cancer Center Director's Award Pilot for Expanded Research), and the South Shore Action for Hope (to R.G.R.).

AUTHOR CONTRIBUTIONS

Z.L., S.F., M.T., K.F., C.-C.C., C.C., and D.W. performed research, M.F., P.C., K.L., T.L., and Q.Z. performed analysis of CUT&RUN and transcriptomic data, S.O., H.L., E.L.D.R., S.H., Q.Z., and R.G.R supervised research. R.G.R. wrote the manuscript.

COMPETING INTERESTS

The authors declare no competing interests.

ADDITIONAL INFORMATION

Supplementary information The online version contains supplementary material available at <https://doi.org/10.1038/s41375-024-02428-y>.

Correspondence and requests for materials should be addressed to Shaoyan Hu, Qian Zhu or R. Grant Rowe.

Reprints and permission information is available at <http://www.nature.com/reprints>

Publisher's note Springer Nature remains neutral with regard to jurisdictional claims in published maps and institutional affiliations.

Springer Nature or its licensor (e.g. a society or other partner) holds exclusive rights to this article under a publishing agreement with the author(s) or other rightsholder(s); author self-archiving of the accepted manuscript version of this article is solely governed by the terms of such publishing agreement and applicable law.